

**THERMAL ROTATIONAL LIGHTCURVE OF (1) CERES AT 1.2 MM WAVELENGTH AND SEARCH FOR HCN WITH ALMA.** Jian-Yang Li<sup>1</sup>, Arielle Moullet<sup>2</sup>, Timothy N. Titus<sup>3</sup>, Mark V. Sykes<sup>1</sup>, Henry H. Hsieh<sup>1</sup>, <sup>1</sup>Planetary Science Institute, Tucson, AZ ([jyli@psi.edu](mailto:jyli@psi.edu)), <sup>2</sup>SOFIA/USRA, Moffett Field, CA, <sup>3</sup>US Geological Survey, Flagstaff, AZ.

**Introduction:** Recent observations of Ceres by NASA's Dawn spacecraft suggested that this dwarf planet is strongly affected by water (ice and/or hydrates) on its surface and crust [1]. The prevalent distribution of ammoniated phyllosilicates suggests a widespread aqueous alteration in Ceres' interior [2,3]. Abundant hydrogen most likely reveals a global distribution of water ice and/or hydration beneath the surface, more abundant at mid- to high-latitude [4]. A few kilometer-sized water ice patches are identified in isolated regions associated with young craters [5]. Pitted terrains [6] and flow-like geomorphological features [7] are additional indicators of abundant water ice in the shallow subsurface. Although conflicting evidence exists about the amount of water ice contained in Ceres' crust [8,9], it is clear that the present physical properties on the surface of Ceres are strongly affected by water ice, and are very different from "dry" asteroids such as Vesta. Therefore, it is key to understand the thermal environment on and beneath the surface of Ceres in order to determine the existence, current state, and the past of surface and near surface water ice.

In order to determine its thermal properties, we imaged Ceres with the Atacama Large Millimeter/sub-millimeter Array (ALMA) in three epochs in October/November 2015, September 2017, and October 2017 with the highest spatial resolution achievable for Ceres under the configuration schedule in each ALMA cycle. The phase angles of Ceres were around 20° during all observations, suggesting that the total thermal flux is dominated by the sub-solar region, although the terminator should be in view. The observations were performed with the 12 m array in Band 6 continuum (frequency 256 GHz) in all three epochs, and also with the ACA in the October 2017 epoch in a spectral configuration that covers the HCN (J=3-2) emission line at 265.89 GHz with a velocity resolution of 0.3 km/s. Observations in all three epochs covered nearly a full rotation of Ceres in three to four nights combined. The goal of these observations was to perform a spatially resolved thermal modeling to map out the thermal inertia and layering on the surface of Ceres, in order to identify thermal anomalies that could either be the reservoir of water ice or host water ice in the subsurface. In this abstract, we report the disk-integrated thermal flux lightcurves of Ceres obtained from our observations, as well as the results of HCN search.

**Data and Reduction:** The interferometer data from are first calibrated with the standard calibration process, and then the spatially resolved images of Ceres at 256 GHz continuum were produced in 5 to 10 min time temporal cadence. The flux calibration is performed with the standard calibration procedure with quasars as the flux standard. The total flux of Ceres is measured by integrating all the pixels in the box just enclose the disk of Ceres. The ACA lightcurve was generated by averaging the correlation data over all spectral bands and all antenna pairs for both polarization directions at a temporal resolution of 30 s. The ACA spectral data were produced by averaging over all data points for each spectral channel. Note that the total power of Ceres measured from the ACA is much more stable than that from the 12 m array in extended configurations, therefore the lightcurve shape of Ceres from ACA data is more reliable than that from the 12 m data.

**Preliminary Results:** The rotational lightcurves of Ceres obtained from all three epochs as well as the ACA in the third epoch are shown in Fig. 1. The peak-to-peak amplitude of the lightcurve is about 3.5%, consistent with the previous observations from Submillimeter Array [10] and Heinrich-Hertz-Telescope [11], but much smaller than that reported by [12], all in comparable frequency. The lightcurve shows a rough double-peaked shape, with a dip at about 240° longitude and possibly another one at about 40° longitude. The phasing of the 256 GHz thermal lightcurve of Ceres is similar to that of the lightcurve in the visible wavelengths [13]. Given that the difference between the two equatorial axes of Ceres is only about 0.4% [14], the rotational variation of total flux should not be dominated by the shape. The relative phasing of the reflected and thermal lightcurves suggests that the thermal lightcurve cannot be dominated by albedo variations. In addition, the low Bond albedo of Ceres of about 3.7% [15] and the small variations of 4% in its reflected lightcurve also suggest that albedo variation cannot be the reason for the thermal flux variations. Therefore, the thermal lightcurve must be an indication of thermal variations across the surface of Ceres, where either the thermal inertia near 40° and 240° longitude is relatively higher, or the surface near those longitudinal regions is relatively smoother, both resulting in lower daily peak temperature.

The spectrum of Ceres in the HCN (J=3-2) frequency is shown in Fig. 2. No signs of HCN emission

is evident in this spectrum. The noise in the spectrum is about 7 K in the raw data, and about 2 K in the smoothed spectrum with a velocity resolution of 0.56 km/s, matching the maximum thermal velocity on the surface of Ceres. Therefore, the previous tentative detection of HCN [16] is not confirmed with our data.

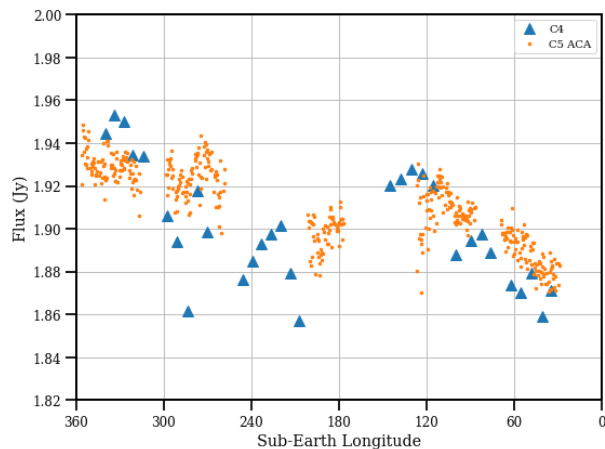


Figure 1. The total thermal flux from Ceres at 256 GHz from the 12 m array in September 2017 epoch (C4) and from ACA in October 2017 (C5 ACA). The C4 lightcurves are normalized to the average geocentric distance in the corresponding epoch. C5 ACA lightcurve is scaled arbitrarily to match the absolute flux level of the C4 lightcurve. The data from the October/November 2015 epoch from the 12 m observations in the October 2017 epoch are not shown due to the large uncertainty in the flux calibration.

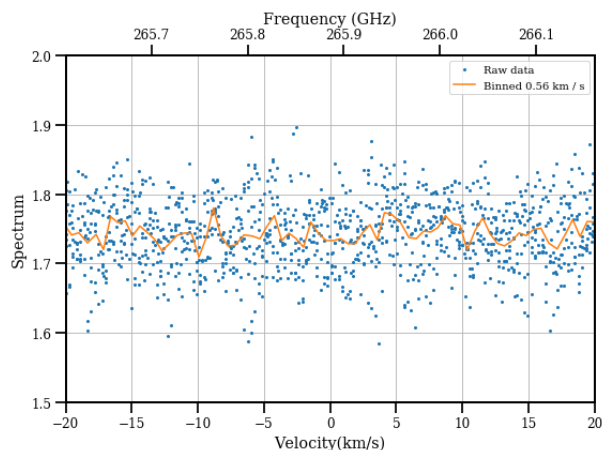


Figure 2. The spectrum of Ceres in the HCN ( $J=3-2$ ) frequency range. The dots are raw spectrum, and the orange line is smoothed with a velocity resolution of 0.56 km/s. No signs of HCN emission line is evident.

**Acknowledgement:** This work is supported by NASA SSO program Grant # NNX15AE02G.

**References:** [1] Sizemore, H.G., et al. (2019) JGR, in revision. [2] De Sanctis, M.C., et al. (2015) Nature 528, 241-244. [3] Ammannito, E., et al. (2016) Science 353, 1006. [4] Prettyman, T.H., et al. (2017) Science 355, 55-59. [5] Combe, J.-P., et al. (2016) Science 353, 1007. [6] Sizemore, H.G., et al. (2017) GRL 44, doi:10.1002/2017GL073970. [7] Schmidt, B.E., et al. (2017) Nature Geosci. 10, 338-343. [8] Bland, M.T., et al. (2016) Nature Geosci. 9, 538-542. [9] Hiesinger, H., et al. (2016) Science 353, 1003. [10] Moullet, A., et al. (2010) AA 516, L10. [11] Altenhoff, W.J., et al. (1996) AA 309, 953-956. [12] Chamberlain, M.A., et al. (2009) Icarus 202, 487-501. [13] Reddy, V., et al. (2015) Icarus 260, 332-345. [14] Russell, C.T., et al. (2016) Science 353, 1008-1010. [15] Li, J.-Y., et al. (2019) Icarus, in press. [16] Kuan, Y.-J. et al. (2016) COSPAR B0.4-79-16.